ORIGINAL RESEARCH

Motor Control, 2010, 14, 323-343

Oscillating in Synchrony with a Metronome: Serial Dependence, Limit Cycle Dynamics, and Modeling

Kjerstin Torre, Ramesh Balasubramaniam, and Didier Delignières

We analyzed serial dependencies in periods and asynchronies collected during oscillations performed in synchrony with a metronome. Results showed that asynchronies contain 1/*f* fluctuations, and the series of periods contain antipersistent dependence. The analysis of the phase portrait revealed a specific asymmetry induced by synchronization. We propose a hybrid limit cycle model including a cycle-dependent stiffness parameter provided with fractal properties, and a parametric driving function based on velocity. This model accounts for most experimentally evidenced statistical features, including serial dependence and limit cycle dynamics. We discuss the results and modeling choices within the framework of event-based and emergent timing.

Keywords: Oscillation, asynchrony, 1/*f* noise, limit cycle model, parametric driving.

So far, studies of single-limb oscillations have essentially focused on oscillators within-cycle dynamics, especially through the analysis of the phase-plane representation of motion. Serial dependence (i.e., cycle-to-cycle dynamics) has been largely disregarded, except in a few studies focusing on self-paced oscillations (Daffertshofer, 1998; Delignières et al., 2004, 2008; Schöner, 1994). Especially, Delignières et al. (2008) revealed the presence of fractal serial dependencies in series of oscillation periods, which could not be accounted for by classical limit cycle models. We focus in the present paper on oscillations performed in synchrony with a metronome. Our first aim was to combine the analyses of within-cycle and cycle-to-cycle oscillation dynamics, to provide a complete characterization of the impact of synchronization on the limb dynamics. In a second step, we propose to assess the capability of some candidate models to account for the empirical results.

Torre is with the Sensorimotor Neuroscience Laboratory, MacMaster University, Canada, and Motor Efficiency and Deficiency, University Montpellier I, France. Balasubramaniam is with the Sensorimotor Neuroscience Laboratory, MacMaster University, Canada. Delignières is with Motor Efficiency and Deficiency, University Montpellier I, France.

Contribution of Serial Correlation Analysis in Tapping Studies

While serial dependence has rarely been studied in the domain of oscillatory motion, it represents a key feature in the related domain of rhythmic finger tapping where the analysis of serial short-range and long-range correlations and their evolution according to experimental manipulations have been considered a crucial step for understanding the underlying processes (Chen, Ding, & Kelso, 1997, Delignières, Torre & Lemoine, 2004, 2008; Gilden, Thornton, & Mallon, 1995; Torre & Delignières, 2008a). With close connection to our present concern, studies contrasting self-paced and synchronized performance have shown typical changes in the correlation structure of experimental time series caused by external pacing.

In this group of tapping studies, the occurrence of long-range correlations, or 1/*f* noise, has been of particular interest. 1/*f* noise defines a very specific temporal structure characterized by persistent dependence between successive observations over time; it has been observed in various rhythmic behaviors (Chen et al., 1997; Delignières et al., 2004; Gilden et al., 1995; Hausdorff et al., 1996; Torre, Delignières, & Lemoine, 2007b). However, the origin and meaning of 1/*f* noise are actual subjects to debate, challenging current theories for motor control. The literature shows two alternative approaches to this issue (Torre & Wagenmakers, 2009). One approach focuses on the theoretical signification and the principles which could clarify the widespread occurrences of 1/*f* noise. Another more domain-specific approach consists in using long-range correlation properties as further statistical criteria for questioning and amending current models of the behavior under study.

The alteration of 1/*f* correlations under some experimental conditions is a key point for investigating the underlying processes. Especially, previous tapping experiments have shown that metronome driving is likely to specifically alter the 1/*f* correlation structure and suggested that serial dependence could offer an interesting window of observation for analyzing the influence of external constraints on timing control processes (Chen et al., 1997; Delignières and Torre, 2009; Hausdorff et al., 1996; Torre & Delignières, 2008a, 2008b).

Focusing on Serial Correlations in Synchronized Oscillations

Regarding single-limb oscillations, the only published experimental results including serial correlation analysis were obtained in self-paced conditions (Daffertshofer, 1998; Delignières et al., 2004, 2008, see also Beek, Peper & Daffertshofer, 2002; Schöner, 1994). Delignières et al. (2004) showed that the series of periods produced by self-paced rhythmic forearm oscillations contained 1/*f* noise, and Delignières et al. (2008) proposed to account for this serial dependence by providing the stiffness parameter of a hybrid self-sustained oscillator (Kay, Saltzman, Kelso, & Schöner, 1987) with 1/*f* fluctuations over successive cycles. This model, and notably the fractal generator that injects long-range dependence in the dynamics of the oscillator, will be detailed in the modeling section of this paper.

Note that the above mentioned results obtained in finger tapping cannot be straightforwardly generalized to oscillatory motion as several studies have supported the idea that tapping and oscillation tasks belong to different classes of rhythmic movement (Delignières et al., 2004, 2008; Robertson et al., 1999; Schöner, 2002;

Spencer, Zelaznik, Diedrichsen, & Ivry, 2003; Zelaznik, Spencer, & Ivry, 2002). Finger tapping is representative of discontinuous movement tasks, involving an event-based form of timing control: A central timekeeper is supposed to determine periodic cognitive events that trigger discrete motor responses. The mechanism of event-based timing has nicely been captured by the well-known Wing and Kristofferson (1973) model. In contrast, continuous movement tasks like oscillations or circle drawing involve an emergent form of timing, exploiting the dynamical properties of movement trajectory (Zelaznik et al., 2002). As a consequence of this distinction between the event-based and emergent forms of timing control, the way in which synchronization is performed in an oscillation task could hardly be inferred from empirical evidences obtained from tapping tasks.

Nevertheless, one could predict that the 1/*f* correlation structure of oscillation periods observed in self-paced condition should be inevitably altered from the moment that oscillations are performed in synchrony with a metronome. Indeed, whatever the discontinuous/continuous character of movement, the series of asynchronies, or errors to the metronome ($ASYN_i$) are the mathematical integration of the series of periods (P_i,) (Chen et al., 1997). As shown by the schematic representation of a synchronization task in Figure 1:

$$P_i = T + ASYN_{i+1} - ASYN_i \tag{1}$$

and

$$ASYN_i = ASYN_0 + \sum_{k=1}^{i} (P_{k-1} - T) \tag{2}$$

where *T* represents the (constant) period of the metronome.

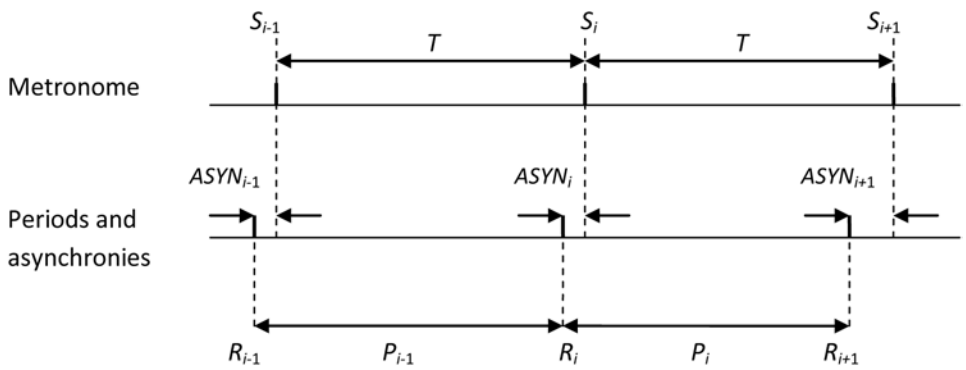

Figure 1 — Schematic representation of the synchronization task. The metronome emits signals S_i, according to a fixed period *T*. Responses (R_i) are separated by periods P_i. Asynchronies ($ASYN_i$) are defined as the time interval between responses and corresponding metronome signals.

At this point it is important to notice that the correlation properties of a given series is theoretically linked to the correlation properties of its differenced or integrated counterparts (for details see Delignières et al., 2006). In particular, the integration of 1/*f* noise corresponds to persistent fractional Brownian motion, a typically nonstationary series. Therefore, if periods in synchronization were still 1/*f* noise, asynchronies would be highly nonstationary which is inconsistent with the essence of synchronized performance. The production of a stable (stationary) performance in terms of asynchronies implies that the corresponding series of periods present antipersistent serial dependence.

This prediction is consistent with the results obtained in finger tapping by Chen et al. (1997) and Torre and Delignières (2008a). The authors evidenced 1/*f* fluctuations in intertap interval series in a self-paced tapping task. In the synchronization condition 1/*f* fluctuations were seen in the series of asynchronies to the metronome, and intertap interval series became antipersistent. Delignières and Torre (2009) showed a similar pattern of results in the analysis of series of stride intervals and asynchronies collected during self-paced and metronomic walking. In both cases, the most intriguing phenomenon was the simultaneous presence of 1/*f* fluctuations in both self-paced and synchronization conditions, but in different aspects of performance (series of periods in the first case, and series of asynchronies in the second).

Chen et al. (1997) suggested that the synchronization process could induce 1/*f* fluctuations by itself. In this view, self-paced and synchronized movements are appraised separately, as distinct processes are assumed to be responsible for the 1/*f* noise observed in self-paced tapping periods on one hand, and in asynchronies in synchronized tapping on the other hand.

Torre and Delignières (2008a) proposed another hypothesis, according to which the process which causes 1/*f* fluctuation in self-paced conditions (as the fractal central timekeeper in the case of tapping) is supposed to continue working in synchronization. However these correlations expresses differently in synchronization, because of coupling to the metronome. In this perspective, self-paced and synchronized movement conditions have to be assessed jointly, as the origin of 1/*f* noise is supposed to be in some process which is common to self-paced and synchronized performances.

The aim of the present article was to analyze the effect of synchronization on forearm oscillations, i.e., an emergent timing task, to determine whether synchronization is achieved in a similar or different way than in finger tapping, i.e., an event-based timing task. In a first step, we present an experiment where participants produced self-paced and synchronized forearm oscillations. We propose a thorough analysis of oscillations in both conditions, including within-cycle dynamics and serial correlations. Our results are discussed in comparison with previous findings in event-based timing tasks. Finally, we tested several candidate models to account for our experimental effect of synchronization on oscillations' serial correlations and within-cycle dynamics.

Experiment

Procedure

Data used here were obtained as part of a larger study, crossing unimanual and bimanual performances of rhythmic finger tapping and forearm oscillations, in self-paced and synchronized movement conditions (Torre & Delignières, 2008b). In the present paper we focus on data obtained in unimanual self-paced and synchronized oscillations.

Participants and Experimental Design

12 participants (mean age 29.0 ± 7.2) were involved in the experiment. None of them had particular expertise or extensive practice in music. They declared no recent upper limb traumatism or neurological injury. They signed an informed consent form, and were not paid for their participation.

The experiment was individually performed in a quiet room. Participants were sitting on a chair with their elbows supported on each side of the body. In the two conditions, participants performed pronation-supination oscillations by manipulating with their dominant hand a 15-cm wooden joystick with a single degree of freedom in the frontal plane. At the beginning of the experiment, the position of the joystick was adjusted to participants' comfort. The required movement frequency was of 2 Hz. For self-paced oscillations, this frequency was initially presented using a 30-s video sequence showing the required forearm oscillations, during which the participants did not perform any movement. Immediately after the video they had to perform oscillations following the prescribed tempo as accurately and regularly as possible, without any feedback. In the synchronization condition, participants had to perform the oscillations in synchrony with PC-driven auditory signal delivered at a frequency of 2 Hz. They were instructed to synchronize the pronation reversals with the signals. In both the self-paced and synchronization conditions they were asked to perform regular oscillations, with an amplitude of about 45 degrees on each side of the central (vertical) position of the joystick. The angular movements were recorded using a potentiometer (Radiospares, 20-K resistance and 25% linearity) located at the axis of the joystick, with a sampling frequency of 300Hz. The trials were pursued up to the recording of 600 successive cycles (each trial lasted about 5 min). Note that the 8 task conditions (one trial in each condition) of the complete experimental design (tapping *vs* oscillation, self-paced *vs* synchronized, and unimanual *vs* bimanual), were performed in random order by each participant.

The analyses that we intended to perform require that the system behaves in steady state during the whole period of observation. Participants were therefore requested to stay concentrated during the whole trials to ensure performance stability. This was particularly important for avoiding any drift in time series in the self-paced condition but less crucial in synchronization conditions where the metronome stabilized the outcome series to achieve stationarity.

Analyses

Data Reduction. A bidirectional low-pass Butterworth filter (cut-off frequency 15 Hz) was applied to the collected voltage data. The successive peaks of the obtained waveform series (corresponding to maximal pronation) were then detected and their times recorded as time series. The variables of interest were series of periods and asynchronies. Periods were computed as the differences between two successive maximal pronation times. Asynchronies were defined as the difference between the times of the maximal pronation and the corresponding auditory signals.

Serial Dependence. For each series, we applied four complementary analyses aiming at a thorough characterization of serial dependence. We first examined the spectral properties of series using ${}^{low}PSD_{we}$ (Eke et al., 2000), an improved version of the classical spectral analysis. The spectral exponent β was estimated by the negative of the linear regression slope of the power spectrum in bilogaritmic coordinates. As proposed by Eke et al. (2000) we excluded the high-frequency power estimates ($f > 1/8$ of maximal frequency) for the fitting of β. $1/f$ fluctuations (i.e., persistent long-range correlations) are characterized by β exponents ranging from 0.5 to 1.5, and negative exponents reveal antipersistent (negative) correlation in the series. Note that in the latter case correlations are not considered long-range correlations (Diebolt & Guiraud, 2005).

Secondly, we applied *Detrended Fluctuation Analysis* (DFA, Peng, Havlin, Stanley, & Goldberger, 1995), working in the time domain. This method is based on the analysis of the relationship between the mean magnitude of fluctuations in the series and the length of the intervals over which these fluctuations are determined. For a fractal series, a power-relationship characterized by the scaling exponent α is expected between the mean magnitude of fluctuations and the length of the interval over which these fluctuations are observed. $1/f$ fluctuations are characterized by α exponents ranging from 0.75 to 1.25. Exponents comprised between 0 and 0.5 reveal antipersistent correlation in the series.

Thirdly, we used ARFIMA/ARMA modeling (*Auto-regressive Fractionary Integrated Moving Average*, see for details Wagenmakers, Farrell & Ratcliff, 2004; Torre, Delignières & Lemoine, 2007a) to evaluate the statistical evidence for the presence of long-range correlation in the series. ARFIMA models contain a process of fractional integration that provides series with long-range dependence properties. In contrast, ARMA models present only short-term dependence (determined by the auto-regressive or moving average processes included in the model). The method consists in fitting 18 models to the studied series: nine are ARMA (p,q) models, p and q varying systematically from 0 to 2, and the other nine are the corresponding ARFIMA (p,d,q) models. In these notations p and q represent the orders of the autoregressive and the moving average processes, respectively, and d is the fractional integration parameter. The best model is selected on the basis of a goodness-of-fit statistic that assesses the trade-off between accuracy and parsimony: the best model is the one that gives a good account of the data with a minimum number of free parameters. We used the Bayes Information Criterion (BIC), which was proven to be the most reliable for detecting long-range dependence (Torre et al., 2007a). The selection of an ARFIMA model provides a statistical evidence for the presence of $1/f$ fluctuations in the series.

Finally, we computed the auto-correlation function of series, from lag 1 to lag 30. Auto-correlation functions offer a qualitative complement to the previous analyses. Especially, long-range correlated series are featured by a slow, power-law decay of correlation over time; in contrast, short-range correlated series exhibit a very rapid exponential decay of the autocorrelation function.

Limit-Cycle Dynamics. To obtain a clear characterization of limit cycle dynamics, we summarized each trial in a normalized average cycle, following the procedure adopted by Mottet and Bootsma (1999), and Nourrit, Delignières, Caillou, Deschamps and Lauriot (2003). We retained for this analysis the 10,000 first points of each collected position series (corresponding to 33.33 s, and approximately 66 oscillation cycles). Each cycle was normalized in time using 150 equidistant points, by means of linear interpolation, and rescaled within the interval [-1,+1]. Point-by-point averaging of these normalized cycles allowed computing a normalized average cycle of 150 points. The first derivative was then computed from this average cycle, and rescaled within the interval [-1, +1]. The limit cycle was portrayed by plotting average velocity against average position. This analysis was performed for both self-paced and synchronized oscillation series.

Results

Serial Dependence

Periods in Self-Paced Oscillations. The mean period was 493 ms, with a mean within-series standard deviation of 19 ms. An example of individual series is portrayed in Figure 2 (left column, upper graph). The log-log power spectrum presented a negative linear regression slope in low frequencies and flattened in high frequencies (Figure 2, left column, middle graph). The mean β exponent was 1.11 ($\pm$ 0.43). DFA yielded a mean α of 0.86 ($\pm$ 0.18). ARFIMA/ARMA modeling confirmed statistically that series were 1/*f* noise, detecting long-range correlation in all series. The auto-correlation function presented a positive auto-correlation at lag one (about 0.20), and then a slow decay with increasing lags (Figure 2, left column, bottom graph). Note that even though the auto-correlation looks visually higher at lag 2 than at lag 1, a repeated-measures ANOVA performed on the three first lags showed no significant differences ($F(2,22) = 1.21$; $p = .32$).

Asynchronies in Synchronization. The mean asynchrony was -10.90 ms, with a mean within-series standard deviation of 42.11 ms. An example individual series is portrayed in Figure 2 (middle column, upper graph). $^{low}PSD_{we}$ yielded a linear regression over the entire range of frequencies in the log-log power spectrum (Figure 2, middle column, middle graph). The mean β exponent was 0.78 ($\pm$ 0.34). DFA confirmed this result with the obtaining of a perfectly linear diffusion plot, with a mean α of 0.87 ($\pm$0.15). ARFIMA/ARMA modeling detected long-range correlation for 9 participants out of 12. Finally, the mean auto-correlation function presented a very slow decay over time (Figure 2, middle column, bottom graph), typical of long-range dependence in series.

Periods in Synchronization. The mean period was 498.73 ms, with a mean within-series standard deviation of 17.42 ms. An example individual series is

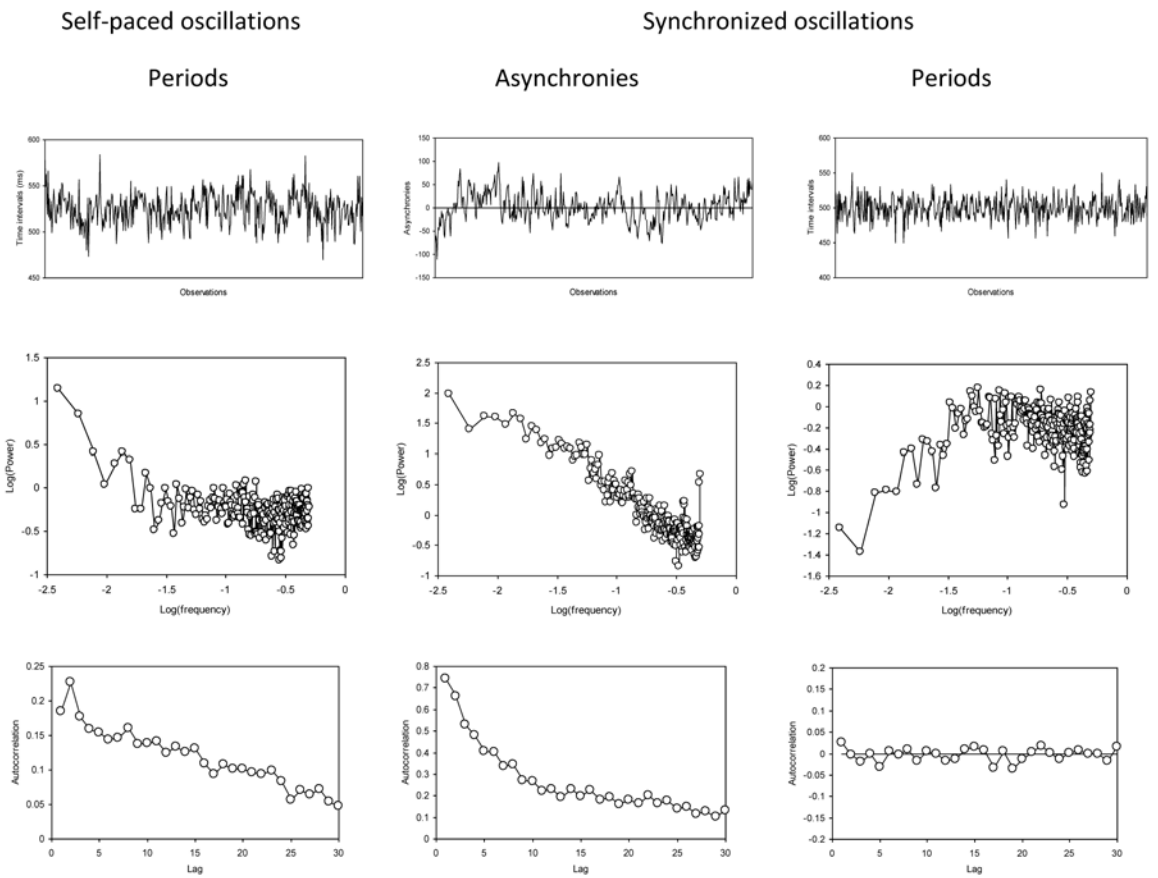

Figure 2 — Graphical results obtained from experimental data in self-paced oscillations and synchronized oscillations. Upper graphs: representative example of individual series. Middle graphs: averaged log-log power spectra. Bottom graphs: averaged auto-correlation functions.

portrayed in Figure 2 (right column, upper graph). $^{low}PSD_{we}$ provided log-log power spectra characterized by a linear, positive slope in the low frequency region, and a flattened slope in high frequencies (Figure 2, right column, middle graph). The mean β exponent was -1.03 ($\pm$ 0.64), and DFA yielded a mean α of 0.31 ($\pm$0.22), showing consistently that series were antipersistent noise. Finally, the mean autocorrelation function presented values close to zero, for the whole range of examined lags (Figure 2, left column, bottom graph).

Limit Cycle Dynamics. Figure 3 (upper graphs) displays the phase portraits of two single series obtained in self-paced (left) and synchronized (right) oscillations. An anchoring effect (i.e., a decrease of the spatial variability of movement cycles revealed by the thinning of the phase plane trajectory) is visible on the right side of the synchronization cycle which corresponds to the occurrence of the metronome signals. Figure 3 (bottom graphs) also presents the normalized average

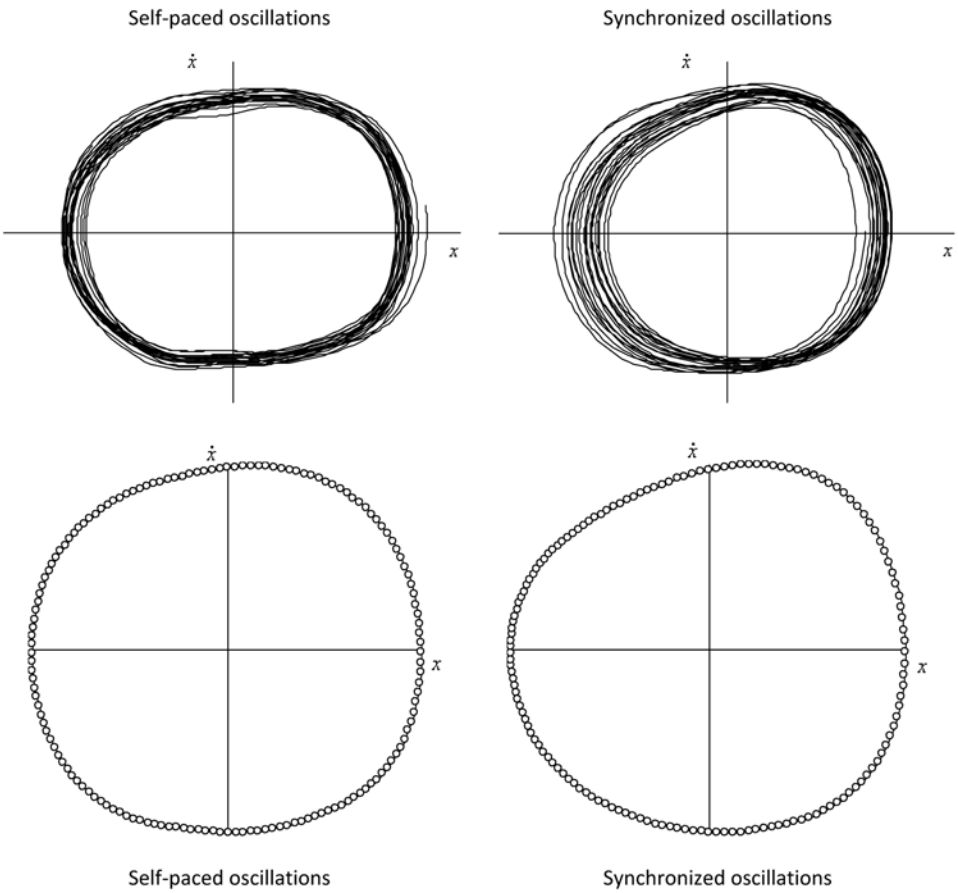

Figure 3 — Limit-cycle dynamics of experimental self-paced and synchronized oscillations. Upper graphs: example individual limit cycles. Bottom graphs: normalized average limit cycles (N = 12).

cycles obtained for the two conditions. Note that these cycles were averaged over the 12 participants, but all individual cycles presented similar shapes. At first glance, the average cycle in self-paced oscillations looked symmetric and circular. In synchronized oscillations, in contrast, an asymmetry appeared between the 'out' phase (semicycle departing from the reversal on the metronome) and the 'back' phase (semicycle toward the metronome) of oscillation cycles. The former (negative velocity values, from the right to the left) was quasi-circular with, nevertheless, a slight shift of the (negative) peak velocity in the first part of the semicycle. The latter (positive velocity values, from the left to the right) presented a stronger deformation, with a delayed peak velocity, occurring in the second part of the semicycle. Note that despite this asymmetry, the two parts of the cycle presented statistically equivalent durations (out: 250 ms ±11; back: 250 ms ±12), and were not mutually correlated (r = -0.06). We finally observed a significant negative correlation between the back phase of the cycle and the preceding asynchrony (r = -0.37, $p < .05$).

Discussion

Previous studies showed that the series of periods obtained in self-paced oscillation and tapping tasks are featured by similar persistent long-range correlations despite some discrepancies due to the different forms of timing control engaged in the two tasks (Delignières et al., 2004, 2008). Our present results show that the similarity between long-range correlation structures of oscillations and tapping also holds in synchronized performance: Oscillating in synchrony with a metronome induces a major alteration of the correlation structure of oscillation periods which turn into antipersistent noise, in the same way as previously shown for synchronized tapping (Chen et al., 1997; Torre & Delignières, 2008a). Moreover, asynchronies were consistently characterized as 1/*f* noise by the different complementary methods of serial correlation analysis. In contrast, the present results differ from previous synchronization tapping results with regard to short-range correlations: For self-paced oscillation periods as synchronized oscillation periods, results showed a flattening of the log-log power spectrum in the high frequencies. Such flattening slope has been considered as the typical signature of emergent timing processes (Delignières et al., 2004) as opposed to the positive slope that is typically observed in tapping.

In tapping, synchronization has been conceived a discrete auto-regressive process, correcting the following period on the basis of the current asynchrony (Vorberg & Schulze, 2002; Vorberg & Wing, 1996). Vorberg and Wing (1996) showed analytically and by means of numerical simulation that this auto-regressive correction process should result in an accentuated negative lag-one auto-correlation in the series of periods; this result has actually been shown in experimental synchronization tapping data (Chen, Ding, & Kelso, 1997; Torre and Delignières, 2008a; Semjen, Schulze & Vorberg, 2000). The present results show that this specific signature of linear phase correction is absent in synchronized oscillations, and allow to reject the hypothesis of a discrete correction process.

An alternative hypothesis for rhythmic movement synchronization suggests that synchronization is achieved through a continuous coupling of the effector, conceived as a self-sustained oscillator, to the metronome (Jirsa, Fink, Foo & Kelso,

2000; Schöner & Kelso, 1988). From this point of view, the specific deformation of the limit cycle we observed between self-paced and synchronized oscillations could provide essential information about the actual nature of this coupling process.

At this point it seems important to clarify that we are not arguing that deformations of the limit cycle necessarily imply the involvement of continuous coupling. Indeed, Balasubramaniam et al. (2004) analyzed the effect of synchronization on the within-cycle dynamics in an 'air tapping' task where participants performed rhythmic taps without any mechanical contact. The data clearly showed the presence of an event-based mode of control, with a discrete error correction process in synchronization condition (see also Balasubramaniam, 2006; Torre & Balasubramaniam, 2009). With regard to the within-cycle dynamics, Balasubramaniam et al. (2004) showed that in the self-paced condition the movements of the finger were quasi-harmonic and symmetrical. In contrast, the kinematic profiles in synchronization condition showed a marked asymmetry, with a slow 'out' phase (semicycle departing from the metronome) and a rapid 'back' phase (semicycle to the metronome). The durations of these two semicycle were negatively correlated (r = -.69), and the degree of correlation was closely linked to the accuracy of synchronization. Finally, the 'out' phase was negatively correlated with the preceding asynchrony (r = -.63), suggesting that this semicycle represents a 'corrective' phase implementing the underlying error correction process (Vorberg & Schulze, 2002; Vorberg & Wing, 1996).

Our present results show a completely different picture. Despite a slight asymmetry between the 'out' and 'back' trajectories, the durations of the two phases were neither statistically different nor correlated. Moreover, we evidenced a negative correlation between the 'back' phase of cycles and the preceding asynchronies which contrasts with the results by Balasubramaniam et al. (2004). The comparison of the phase plot presently obtained in synchronized oscillations and that presented by Balasubramaniam and collaborators (see Figure 1, right column, second graph from the top in Balasubramaniam et al., 2004) clearly suggests that two different synchronization processes are involved in the two tasks.

Our results regarding limit cycle dynamics, and in particular the smooth and continuous deformation that appeared with synchronization to the metronome, support the hypothesis that synchronization is achieved on the basis of a continuous coupling process. However, the relative contributions of the oscillator's intrinsic dynamics and the coupling function remain to be clarified. We propose to address this issue in the following modeling section. In this view, the present empirical characterization of the impact of synchronization on single-limb oscillations with regard to serial dependence and limit-cycle dynamics provides a demanding set of criteria for assessing candidate models.

Modeling

The dynamics of a single oscillating effector has classically been modeled by a hybrid differential equation, associating Rayleigh and van der Pol damping terms (Kay et al., 1987):

$$\ddot{x} = \alpha\dot{x}\text{-}\beta\dot{x}x^2 - \gamma\dot{x}^3 - \omega^2 x \tag{3}$$

This equation describes the intrinsic dynamics of a self-sustained oscillator whose frequency is mainly determined by the linear stiffness term ω^2. This model provides a satisfying account for the empirical relationships between frequency, amplitude, and peak velocity during self-paced limb oscillations (Kay et al., 1987).

Schöner and Kelso (1988) conceived the metronome as an environmental information attracting the dynamics of the effector toward the prescribed frequency. They proposed to add a linear cosine term to drive the limit cycle oscillator. Jirsa et al. (2000) further showed that a more complex model including a parametric driving term is more appropriate to account for the specific influence of external pacing on the limit cycle dynamics. The simplest formulation of the parametric driving model obeys the following equation (Fink et al., 2000; Assisi et al., 2005):

$$\ddot{x} = \alpha\dot{x} - \beta\dot{x}x^2 - \gamma\dot{x}^3 - \omega^2 x + \varepsilon_1 \cos\Omega t + \varepsilon_2 \cos\Omega t \qquad (4)$$

where Ω is the frequency at which the metronome is presented and ε_1 and ε_2 are the strengths of the linear and parametric driving terms, respectively. Contrary to the linear driving model of Schöner and Kelso (1988), the parametric driving model accounted for the decrease of spatial variability in the phase plane at the anchored point (Assisi et al., 2005). However, the criteria used for assessing the validity of this model remained limited in scope, since they focused exclusively on the analysis of the stability properties of limit cycle dynamics.

We first examined the properties of the parametric driving model by Assisi and collaborators (2005). We used the following parameters: $\alpha = .5$, $\beta = 1.0$, $\gamma = 0.02$, $\omega = 4\pi$, $\varepsilon_1 = 0.1$ and $\varepsilon_2 = 3$, and $Q = 0.1$. These parameter values were consistent with those used in recent simulation[1] experiments (Jirsa et al., 2000, Leise & Cohen, 2007). Simulations allowed to reproduce the typical anchoring phenomenon in the limit cycle dynamics. However the model failed to account for the presence of 1/*f* noise in asynchronies. Applying ${}^{low}PSD_{we}$ to simulated asynchrony series yielded a mean β of -0.96 (± 0.21). Consistently, the DFA yielded a mean α of 0.24 (± 0.07), suggesting the presence of antipersistent dependence. This pattern of results confirmed that the parametric driving model was per se unable to generate the persistent long-range correlation pattern observed in the experiment.

In consequence, it seems reasonable to assume that the serial correlation pattern observed in synchronized oscillations emerges from the combination of the oscillator's intrinsic dynamics (characterized in self-paced condition by 1/*f* fluctuations), and the driving function which induces antipersistent dependence. One could argue, nevertheless, that the choice of the driving function was inappropriate for generating the expected correlation pattern. Chen et al. (1997) proposed a coupling function including feedback delays that seemed able to generate by itself 1/*f* fluctuations. This hypothesis, however, cannot account for the presence of 1/*f* fluctuations in both self-paced (periods) and synchronized (asynchronies) conditions, and it remains difficult, from a dynamical point of view, to suggest that the intrinsic (fractal) dynamics of the self-paced oscillator could be completely overridden by a coupling function. Our statement, suggesting that the pattern of correlations arises from the combination of the intrinsic dynamics of the oscillator and the driving function offers an integrative framework for self-paced and synchronized oscillations (for a similar approach to event-based timing, see Torre & Delignières, 2008a). Therefore, a solution is to start with a model accounting for

fractal fluctuations in self-paced oscillations, and to enrich this first model with a synchronization process.

Delignières et al. (2008) proposed a model for accounting for the presence of long-range dependence in self-paced oscillations. The starting point is the hybrid model by Kay et al. (1987) accounting for the dynamics of a single oscillating limb (Eq. 3). A noise term of strength Q is added to this model to simulate the perturbations that affect all dynamical systems. In any case, the original hybrid model is unable to generate the persistent long-range correlations evidenced in self-paced oscillations (Delignières et al., 2008). Seeing that the oscillation periods in this model are mainly determined by the linear stiffness parameter ω^2, Delignières et al. (2008) proposed to provide this parameter with fractal properties over the successive cycles. Such a solution was previously explored by Ashkenazy, Hausdorff, Ivanov and Stanley (2002) and West and Scafetta (2003), in the domain of locomotion: the authors developed the so-called 'hopping' model which was able to generate a fractal series of stiffness values.

The key element of the hopping model is a linear Markov process δ_j, generated by a first-order auto-regressive equation:

$$\delta_j = \phi\delta_{j-1} + \eta\xi_j \tag{5}$$

where $0< \phi <1$ is a constant and ξ_j is a white noise process with zero mean and unit variance. The chain then contains "correlated zones" of typical size r:

$$r = -1/\log\phi \tag{6}$$

Each δ_j could then be considered at the center of a zone of correlated neighbors, the size of which depends on the strength of the auto-regressive process that generated the whole chain. The successive states of the system are supposed to be activated by a random walk along the chain. The size of the successive jumps of this random walk follows a Gaussian distribution of width ρ. This random walk generates a series δ_i, representing the state adopted by the effector for each successive cycle i. In this process, correlations within the δ_i series are assumed to increase with the size of correlation within the chain (r), and to decrease as the width ρ of the distribution of jumps increases.

Finally, the frequency of the limit cycle is determined, for each successive cycle i, by

$$\omega_i = \omega_0 + \mu\delta_i + \theta\xi_i \tag{7}$$

where ω_0 represents the baseline frequency, μ is a constant, and ξ_i is a white noise with zero mean and unit variance. The addition of this white noise process of strength θ to the series of stiffness values was motivated by the observation of the flattening of the log-log power spectrum in the high frequencies (Delignières et al., 2004), suggesting the presence of high-frequency random fluctuations. This series of linear stiffness parameters is then injected into the hybrid model (Eq. 1). Delignières et al. (2008) showed that this model allowed to simulate the $1/f$ structure of periods in self-paced oscillations. Figure 4 (left column) presents the results of this model using $\alpha = 0.5$, $\beta = 1.0$, $\gamma = 0.02$, and $Q = 0.1$ for the hybrid limit cycle

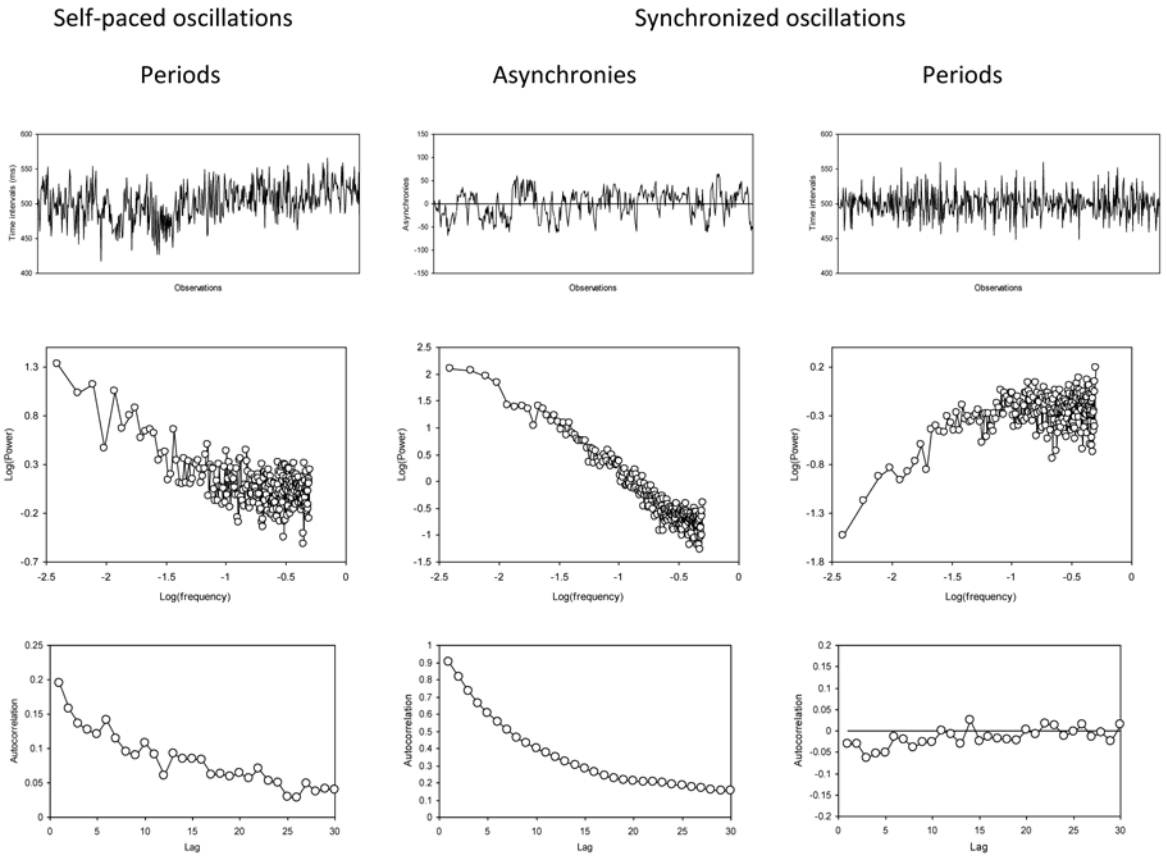

Figure 4 — Graphical results obtained from simulations of self-paced oscillations and synchronized oscillations. Upper graphs: representative example of individual series. Middle graphs: averaged log-log power spectra. Bottom graphs: averaged auto-correlation functions. Power spectra and auto-correlation functions were computed from 12 randomly selected series.

model, and $\omega_0 = 4\pi$, $r = 25$, $\eta = 0.1$, $\rho = 25$, $\mu = 1.0$, and $\theta = 0.01$ for the hopping model. The mean power spectrum and the auto-correlation function were similar to those obtained during the experiment for self-paced oscillations (see Figure 2, left column). The mean β exponent was 0.85 (*SD* = 0.52), and DFA yielded a mean α exponent of 0.82 (*SD* = 0.17). ARFIMA modeling detected long-range dependence in 97% of the simulated series. We display in Figure 5 (left column) an example of the phase-plane representation obtained for one realization of the model, and an average normalized limit cycle, computed over 12 randomly selected realizations.

Given the ability of the parametric driving model to account for some essential aspects of the coupling to the metronome, we analyzed the properties of series generated by a combination of the hopping model and the parametric driving model. In a first step, we used the simplest formulation of the model, including a linear driving term and a position-based parametric driving term (see Eq. 4). This solution yielded a satisfying pattern of serial dependence, with persistent long-range correlations

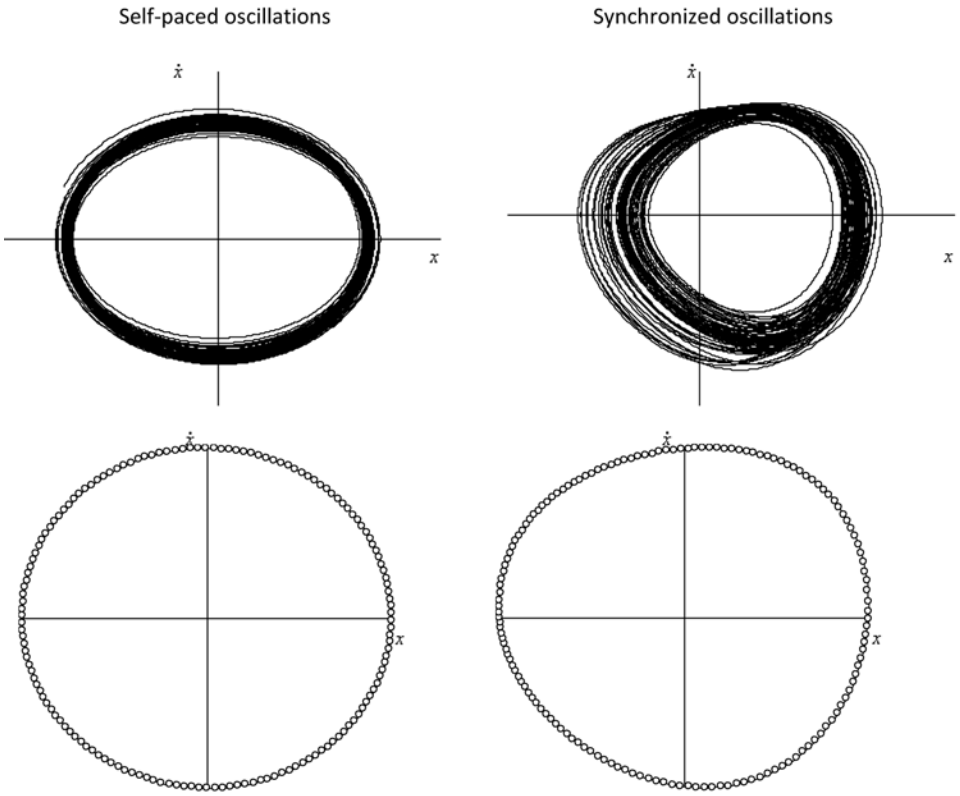

Figure 5 — Limit-cycle dynamics of simulated self-paced (left) and synchronized (right) oscillations. Upper graph: example simulated limit cycles (50 cycles). Bottom graph: normalized average limit cycles, computed from 12 simulated series of 100 cycles.

in asynchronies, and antipersistent correlations in periods. The model moreover produced an asymmetric deformation of the limit cycle, with the characteristic shifts of peak velocities in the two semicycles similar to our experimental results. Nevertheless, the anchoring phenomenon appeared at the opposite reversal point of the cycle (i.e., on the left in our conventions), which discarded this modeling solution (graphical results of this simulation are not presented).

The very specific deformation of the limit cycle observed in experimental series provided a precise criterion to select the most relevant way for modeling synchronization. We tested a number of candidate models, indexing driving to position or to velocity, and using sine or cosine functions. The most parsimonious solution was to use a higher order parametric driving term (indexed on velocity rather than on position), and to use a sine driving function for this term, rather than a cosine function. The change of the cosine to a sine was essential for obtaining the anchoring at the right side of the phase plane. This new synchronization model is written:

$$\ddot{x} = \alpha\dot{x} - \beta\dot{x}x^2 - \gamma x^3 - \omega_i^2 x + \varepsilon_1 \cos\Omega t + \varepsilon_3 \dot{x} \sin\Omega t + \sqrt{Q}\xi_t \quad (8),$$

ω_i fluctuation from cycle to cycle being determined by the hopping model. We used the following model parameters for simulation: $\alpha = 0.5$, $\beta = 1.0$, $\gamma = 0.02$, $\Omega = 4\pi$, $\varepsilon_1 = 0.3$, $\varepsilon_3 = 0.05$, and $Q = 0.1$. The parameters specific to the hopping model were the same than those previously used for the simulation of self-paced oscillation periods.

Using this set of parameters provided satisfying results. The Gaussian properties of the simulated series were similar to the experimental series, with mean asynchrony of -3.50 ms (± 39.07), and a mean period of 499.98 ms (± 0.08). Representative examples of simulated series are presented in Figure 4 (upper graphs, asynchronies: middle column; periods: right column).

Regarding simulated asynchronies, the $^{low}PSD_{we}$ yielded a linear regression in the log-log power spectrum, over the entire range of frequencies (Figure 4, middle column, middle graph). The mean β exponent was 0.93 (± 0.13). DFA gave consistent results with a perfectly linear diffusion plot, and a mean α of 0.93 (± 0.14). ARFIMA/ARMA modeling detected long-range correlation in 88% of series. Finally, the mean auto-correlation function presented a very slow decay over the successive lags (Figure 4, middle column, bottom graph), similar to that obtained with experimental series.

For the simulated periods, as for experimental periods, the $^{low}PSD_{we}$ provided log-log power spectra characterized by a linear, positive slope in the low frequency region, and a flattened zone in high frequencies (Figure 4, right column, middle graph). The mean β exponent was -1.24 (± 0.36), and DFA yielded a mean α of 0.19 (± 0.05). The mean auto-correlation function presented values close to zero, for the whole range of examined lags (Figure 4, right column, bottom graph). Note that visual inspection of the graphs could suggest a negative auto-correlation at the first lags for simulated periods, whereas a positive auto-correlation at the first lag was obtained for experimental series (see Figure 2). However, the auto-correlations were not significant at any lag for both simulated and experimental periods, and there was no significant difference between the lag one auto-correlations from simulated and experimental series ($F(1,11) = 11.55$, $p = .24$).

Finally, Figure 5 (right column, upper graph) displays an example of the limit cycles obtained from simulated series. The anchoring phenomenon clearly appeared

at the oscillator's maximal position. As for the experimental series, there was a significant negative correlation between the durations of the semicycles 'back' and the preceding asynchronies (r = -0.72). We computed an average normalized limit cycle, on the basis of 12 randomly chosen realizations (Figure 5, right column, bottom graph). This average limit cycle clearly exhibited an asymmetry similar to the experimental cycles, with a precocious velocity peak in the 'out' phase and a delayed velocity peak in the 'back' phase. Note that despite the similarities in the positions of the anchor points and the velocity peaks, the shape of the simulated limit cycle is slightly different from the empirical one, suggesting that the latter involved a stronger nonlinear damping. Further investigations could allow a final refinement of the model.

General Discussion

Experimental data allowed us to specify a number of dynamic signatures of self-paced and synchronized forearm oscillations. Results confirmed that the series of periods in self-paced oscillations presented genuine long-range dependence (Delignières et al., 2004). In the synchronization condition, the correlation structure of periods became antipersistent, and 1/*f* fluctuations appeared at the level of asynchronies. These correlation structures were evidenced through the combination of spectral, temporal, and auto-correlation analyses (Delignières et al., 2006), and attested by ARFIMA modeling (Torre et al., 2007a).

These results paralleled those previously obtained in self-paced *versus* synchronized tapping performances. Therefore, they could at first sight seem to support the hypothesis of a similar synchronization process, i.e., a discrete cycle-to-cycle correction of asynchronies, underlying synchronized tapping and oscillations. Basing on a comparison of our present results and those reported by Balasubramaniam et al. (2004) in tapping, we went for a different perspective on synchronization in line with the continuous coupling hypothesis developed by Jirsa et al. (2000).

Simulations allowed to test and refine this continuous coupling hypothesis. First, we showed that the original parametric driving model proposed by Jirsa et al. (2000) was not able to generate the experimentally observed correlation structures. A solution for this problem was to provide the stiffness parameter of the model with fractal properties. By testing different forms of continuous coupling functions we further identified a form of parametric driving based on the oscillator's velocity as the simplest solution to account simultaneously for the empirical cycle dynamics and the serial correlation structure. Combined with the hopping model, this coupling function allowed to generate series reproducing most of the experimentally established signatures. At this point, two points stand naturally out for discussion: (i) the way we chose to provide the oscillator with long-range correlations, and (ii) the way to model the coupling between the limb oscillations and the metronome.

To insert long-range correlations into the synchronized oscillations model, we provided the stiffness parameter of the model with a fractal cycle-to-cycle variability as suggested by West and Scafetta (2003). Therefore, we used the "hopping" model which was proven to generate genuine fractal correlations in the series of periods produced by a limit-cycle model (Delignières et al., 2008). In the domain of human locomotion, West and Scafetta (2003) suggested that this "hopping" model could represent the activity a *central pattern generator*, an intraspinal network of neurons capable of producing a rhythmical output. Note that we do not postulate the presence

of such a central pattern generator in the forearm oscillations involved in the present experiment. Our results show that forearm oscillations and limb oscillations during locomotion share similar statistical features that could reveal a general property of biological oscillators, characterized by a fractal evolution of stiffness over time. This fractal property could represent an essential ingredient for understanding the serial dynamics of limb oscillations. The formal architecture of the hopping model suggests that effectors present a set of possible neighboring states that are determined by similar factors and mutually correlated. A simple random walk among this set could produce the fractal correlation structure observed during repetitive oscillations (Delignières et al., 2008). The biological interpretation of this virtual set of neighboring states remains speculative. One could suggest that the multiple components that compose the system could potentially present a number of different configurations. These configurations could determine some essential properties, and especially effector's stiffness. Different configurations could share some common features, determining these virtual "correlated zones" of neighbor states.

In the present work we followed the modeling strategy proposed by Jirsa et al. (2000), modeling limb motion by a single hybrid oscillator model. This hybrid model was dismissed by Beek et al. (2002), and the authors proposed a system of two coupled oscillators which presented a number of advantages as compared with the hybrid oscillator model: It notably allowed to account for empirically observed nonmonotonic frequency-amplitude relations and phase shifts in response to external perturbations. With respect to serial correlation however, a system of two coupled oscillators seems only able to generate antipersistent short-term correlations (Daffertshofer, 1998). The first simulation we performed on the original parametric driving model (Jirsa et al., 2000), which is essentially a system of coupled oscillators similar to that analyzed by Daffertshofer (1998), confirmed that this kind of model is unable per se to generate long-range correlations. Future investigations should check whether injecting a source of $1/f$ noise in a system of coupled oscillators would allow accounting for our present results while preserving the stability properties of the model.

Regarding the way to model the coupling between limb oscillations and metronomic signals, our simulation section allowed us to deepen previous studies: although we support the idea that parametric driving is necessary for accounting for the anchoring phenomenon in limit cycle dynamics (Jirsa et al., 2000), simulations led us to select a different form of parametric driving than those previously used. Fink et al. (2000) and Assisi et al. (2005) choose to couple metronome input to limb position (Eq. 4), but they suggested that a parametric driving term coupling the stimulus to velocity rather than to position should produce qualitatively similar results (Fink et al., 2000). The present work shows that the position-based coupling function does not allow the specific deformation of the limit cycle observed in experimental synchronization series, while a velocity-based coupling between the oscillator and the stimulus yielded more satisfactory results. As we indicated, this solution appeared as the most simple (i.e., parsimonious) for accounting for our experimental results.

The use of a continuous driving function to account for the effect of a sequence of discrete stimuli might seem counterintuitive and merely *convenient* from a mathematical point of view, although it is clear that the driving function does not model the actual signals of the metronome but the way the oscillations dynamics globally adapts to these temporal constraints. Actually, observing kinematic changes in oscillations induced by the metronome does not necessarily mean that

the coupling between the movement and the metronome is continuous indeed. Nevertheless, the present results show that in the case of oscillations, coupling to the metronome yields qualitatively different kinematic changes than those observed in the tapping experiment by Balasubramaniam et al. (2004) where a discrete correction of asynchronies was involved.

We believe that the issue of modeling synchronized oscillations using a continuous coupling function instead of discrete error correction should not be considered without any regard to the theoretical framework which distinguishes between the event-based and emergent forms of timing control (Delignières et al., 2004, 2008; Robertson et al., 1999; Schöner, 2002; Spencer et al., 2003; Zelaznik et al., 2002). Although there is probably no doubt that a link between timing demands and trajectory dynamics does exist indeed, the nature, or *hierarchy* of this relationship (and as a consequence, the nature of appropriate models) may be conceived differently according to whether one considers event-based or emergent timing. Event-based timing theory assumes a dissociation between the level which is responsible for the representation of timing goals and the level of motor implementation (Wing & Kristofferson, 1973). Then, one may choose to focus either on the way time intervals (absolute, or relative to a metronome) are estimated and controlled (Vorberg & Wing, 1996), or on the way motor implementation adapts and serves these timing goals (Balasubramaniam et al., 2004). In contrast, emergent timing theory considers that timing goals and movement dynamics cannot be assessed separately, as the movement trajectory does not only bring the effector to a given point at the required times t, $t+1$, $t+2$, etc., but temporal regularity arises from the consistency of the oscillator's dynamical properties (Schöner, 2002; Zelaznik et al., 2002). Movement dynamics may be considered as *serving* event-based timing (as it may also serve any other accuracy demand[2]) while it *generates* emergent timing. This suggests that for emergent timing the system is organized in such a way that the influence of the discrete metronome is continuous, given the continuous character of the underlying control process.

Finally, the issue of modeling synchronized movement tasks using a continuous, within-cycle coupling function or a discrete, cycle-to-cycle error correction process also rises a connected issue that needs further investigation: While the autoregressive correction of asynchronies which has usually been assumed in tapping (Vorberg & Schulze, 2002) supposes that the asynchronies are the time intervals supporting information used to synchronize the movement to the metronome, a within-cycle coupling between the movement and the metronome rather suggests that the perceived period of the metronome is the time interval of reference that the movement cycle has to match.

Notes

1. All simulations in this modeling section, were performed using a four-stage Runge-Kutta algorithm, following the scheme described by Burrage, Lenane and Lythe (2007, pp. 11–12), for second-order stochastic differential equations with additive noise, with a fixed step size of 0.001 s 100 series of 512 data points were generated for each proposed model.

2. For example, one may draw an analogy with a study of Fitt's task by Mottet & Bootsma (1999): The authors modeled the reciprocal aiming movement using limit-cycle dynamics and evidenced notably an increasing contribution of the nonlinear stiffness parameter with increasing task difficulty. The changes in the limit-cycle dynamics were assumed to serve the spatial accuracy demands.

References

Ashkenazy, Y., Hausdorff, J.M., Ivanov, P.C., & Stanley, H.E. (2002). A stochastic model of human gait dynamics. *Physica A, 316,* 662–670.

Assisi, C.G., Jirsa, V.K., & Kelso, J.A.S. (2005). Dynamics of multifrequency coordination using parametric driving:theory and experiment. *Biological Cybernetics, 93,* 6–21.

Balasubramaniam, R. (2006). Trajectory formation in timed rhythmic movements. In M.L. Latash & F. Lestienne (Eds.), *Progress in Motor Control IV* (pp. 47–54). New York: Springer.

Balasubramaniam, R., Wing, A.M., & Daffertshofer, A. (2004). Keeping with the beat: movement trajectories contribute to movement timing. *Experimental Brain Research, 159,* 129–134.

Beek, P.J., Peper, C.E., & Daffertshofer, A. (2002). Modeling rhythmic interlimb coordination: Beyond the Haken-Kelso-Bunz model. *Brain and Cognition, 48,* 149–165.

Burrage, K., Lenane, I., & Lythe, G. (2007). Numerical Methods for second-order stochastic differential equations. *SIAM Journal on Scientific Computing, 29,* 245–264.

Chen, Y., Ding, M., & Kelso, J.A.S. (1997). Long memory processes ($1/f^{\alpha}$ type) in human coordination. *Physical Review Letters, 79,* 4501–4504.

Daffertshofer, A. (1998). Effects of noise on the phase dynamics of nonlinear oscillators. *Physical Review E: Statistical Physics, Plasmas, Fluids, and Related Interdisciplinary Topics, 58,* 327–338.

Delignières, D., & Torre, K. (2009). Fractal dynamics of human gait: a reassessment of the 1996 data of Hausdorff et al. *Journal of Applied Physiology, 106,* 1272–1279.

Delignières, D., Lemoine, L., & Torre, K. (2004). Time intervals production in tapping and oscillatory motion. *Human Movement Science, 23,* 87–103.

Delignières, D., Ramdani, S., Lemoine, L., Torre, K., Fortes, M. & Ninot, G. (2006). Fractal analysis for short time series : A reassessement of classical methods. Journal of Mathematical Psychology, 50, 525-544.

Delignières, D., Torre, K., & Lemoine, L. (2008). Fractal models for event-based and dynamical timers. *Acta Psychologica, 127,* 382–397.

Diebolt, C., & Guiraud, V. (2005). A note on long memory time series. *Quality & Quantity, 39,* 827–836.

Eke, A., Herman, P., Bassingthwaighte, J.B., Raymond, G.M., Percival, D.B., Cannon, M., et al. (2000). Physiological time series: distinguishing fractal noises from motions. *Pflugers Archiv, 439,* 403–415.

Fink, P.W., Foo, P., Jirsa, V.K., & Kelso, J.A.S. (2000). Local and global stabilization of coordination by sensory information. *Experimental Brain Research, 134,* 9–20.

Gilden, D.L., Thornton, T., & Mallon, M.W. (1995). 1/f noise in human cognition. *Science, 267,* 1837–1839.

Hausdorff, J.M., Purdon, P.L., Peng, C.K., Ladin, Z., Wei, J.Y., & Goldberger, A.R. (1996). Fractal dynamics of human gait: stability of long-range correlations in stride interval fluctuation. *Journal of Applied Physiology, 80,* 1448–1457.

Jirsa, V.K., Fink, P., Foo, P., & Kelso, J.A.S. (2000). Parametric Stabilization of Biological Coordination: A Theoretical Model. *Journal of Biological Physics, 26,* 85–112.

Kay, B.A., Saltzman, E.L., Kelso, J.A.S., & Schöner, G. (1987). Space-time behavior of single and bimanual rhythmical movements: Data and limit cycle model. *Journal of Experimental Psychology. Human Perception and Performance, 13,* 178–192.

Leise, T., & Cohen, A. (2007). Nonlinear oscillators at our fingertips. *The American Mathematical Monthly, 114,* 14–28.

Mottet, D., & Bootsma, R.J. (1999). The dynamics of goal-directed rhythmical aiming. *Biological Cybernetics, 80,* 235–245.

Nourrit, D., Delignières, D., Caillou, N., Deschamps, T., & Lauriot, B. (2003). On discontinuities in motor learning: A longitudinal study of complex skill acquisition on a ski-simulator. *Journal of Motor Behavior, 35,* 151–170.

Peng, C.K., Havlin, S., Stanley, H.E., & Goldberger, A.L. (1995). Quantification of scaling exponents and crossover phenomena in non stationary heartbeat time series. *Chaos (Woodbury, N.Y.), 5,* 82–87.

Robertson, S.D., Zelaznik, H.N., Lantero, D.A., Bojczyk, G., Spencer, R.M., Doffin, J.G., et al. (1999). Correlations for timing consistency among tapping and drawing tasks: evidence against a single timing process for motor control. *Journal of Experimental Psychology. Human Perception and Performance, 25,* 1316–1330.

Schöner, G. (1994). From interlimb coordination to trajectory formation: common dynamical principles. In S. Swinnen, H. Heuer, J. Massion, & P. Casaer (Eds.), *Interlimb coordination: Neural, dynamical and cognitive constraints* (pp. 339–368). San Diego: Academic Press.

Schöner, G. (2002). Timing, clocks, and dynamical systems. *Brain and Cognition, 48,* 31–51.

Schöner, G., & Kelso, J.A.S. (1988). A synergetic theory of environmentally-specified and learned patterns of movement coordination: I. Component oscillator dynamics. *Biological Cybernetics, 58,* 81–89.

Semjen, A., Schulze, H.H., & Vorberg, D. (2000). Timing precision in continuation and synchronisation timing. *Psychological Research, 63,* 137–147.

Spencer, R.M.C., Zelaznik, H.N., Diedrichsen, J., & Ivry, R.B. (2003). Disrupted timing of discontinuous but not continuous movements by cerebellar lesions. *Science, 300,* 1437–1439.

Torre, K. & Balasubramaniam, R. (2010). Two different processes for sensorimotor synchronization in continuous and discontinuous rhythmic movements. Experimental Brain Research, 199, 157-166.

Torre, K., Delignières, D., & Lemoine, L. (2007a). Detection of long-range dependence and estimation of fractal exponents through ARFIMA modeling. *The British Journal of Mathematical and Statistical Psychology, 60,* 85–106.

Torre, K., Delignières, D., & Lemoine, L. (2007b). 1/*f* β fluctuations in bimanual coordination: An additional challenge for modeling. *Experimental Brain Research, 183,* 225–234.

Torre, K., & Delignières, D. (2008a). Unraveling the finding of 1/fβ noise in self-paced and synchronized tapping: A unifying mechanistic model. *Biological Cybernetics, 99,* 159–170.

Torre, K., & Delignières, D. (2008b). Distinct ways for timing movements in bimanual coordination tasks: The contribution of serial correlation analysis and implications for modeling. *Acta Psychologica, 129,* 284–296.

Torre, K., & Wagenmakers, E.J. (2009). Theories and models for 1/f noise in human movement science. *Human Movement Science, 28,* 297–318.

Vorberg, D., & Schulze, H.H. (2002). Linear phase-correction in synchronization: Predictions, parameter estimation, and simulations. *Journal of Mathematical Psychology, 46,* 56–87.

Vorberg, D., & Wing, A. (1996). Modeling variability and dependence in timing. In H. Heuer & S.W. Keele (Eds.), *Handbook of perception and action* (Vol. 2, pp. 181–262). London: Academic Press.

Wagenmakers, E-J., Farrell, S., & Ratcliff, R. (2004). Estimation and interpretation of 1/*f*α noise in human cognition. *Psychonomic Bulletin & Review, 11,* 579–615.

West, B.J., & Scafetta, N. (2003). Nonlinear dynamical model of human gait. *Physical Review E: Statistical, Nonlinear, and Soft Matter Physics, 67,* 051917.

Wing, A.L., & Kristofferson, A.B. (1973). The timing of interresponse intervals. *Perception & Psychophysics, 13,* 455–460.

Zelaznik, H.N., Spencer, R.M., & Ivry, R.B. (2002). Dissociation of explicit and implicit timing in repetitive tapping and drawing movements. *Journal of Experimental Psychology. Human Perception and Performance, 28,* 575–588.